

## NEUTRON IRRADIATION EFFECTS ON ALLOY SUPERCONDUCTORS

H.W. WEBER

*Atominstiut der Österreichischen Universitäten, A-1020 Wien, Austria*

Received 8 January 1982; accepted 1 February 1982

A review of neutron irradiation effects on alloy superconductors, in particular NbTi, is presented. In these materials superconductivity is influenced predominantly by defect-induced changes of the microstructure, which is responsible for flux pinning. Because detailed studies of flux-pinning mechanisms in commercial materials are still scarce, an attempt is made to classify the materials according to their thermomechanical treatment, the corresponding bulk-pinning curves and some electron-microscopic work and to establish correlations with subsequent neutron irradiation effects. In addition, the influence of irradiation temperature, thermal cycling and stabilizer performance are presented and discussed in view of their relevance for fusion reactor applications.

### 1. Introduction

There is general agreement today that, for economic reasons, the magnets needed to confine the high-energy plasma in fusion reactors will have to be superconducting. This implies that the superconducting material selected for the magnet fabrication has to meet a combination of rather severe working conditions: magnetic fields in the 8-12 T range have to be produced reliably over the lifetime of the plant (say 30 years) in the presence of high mechanical stresses and asymmetric forces, pulsed magnetic fields, occasional temperature excursions or complete thermal cycles to room temperature and a special environment of high-energy neutron and gamma irradiation.

The combined influence of all of these parameters on the conductor performance is still far beyond the present state of material testing programs. However, spurred by the development of fusion concepts and programs, some of these aspects have received considerable attention during the past few years. One of these is the influence of radiation environments on candidate magnet components, where most of the work has been concentrated on the response of the superconducting material itself [1,2]. It was recognized, however, that synergistic effects of irradiation and mechanical stress [3], degradation of the stabilizing materials [4-6] and, in particular, the performance of insulators [4,5,7] deserved more attention.

This paper is intended to review the work on neutron

irradiation effects in today's most commonly used magnet material NbTi. Neutron irradiation effects in compounds (A15's and non-A15's) as well as charged particle irradiation of all superconductors will be covered by other contributions to this conference [8,9]. In the following sections I will briefly discuss the neutron spectra which are expected to occur at the location of the magnet, compare them with those of typical test facilities and mention the nature of the defects produced in the superconductor at different irradiation temperatures (section 2). I will then try to summarize the flux-pinning mechanisms in NbTi, which determine the magnitude of the critical current density (section 3). Section 4 is devoted to a survey of experimental results on the changes of  $j_c$  obtained under various irradiation conditions. The conclusions presented in section 5 will show (unfortunately) that sufficiently accurate answers to questions which may be raised by an engineer are still not at hand.

### 2. Neutron spectra and defect production

The neutrons produced by the DT reaction have energies between about 10 and 18 MeV with a sharp peak at the reaction energy of 14.08 MeV. This original neutron spectrum incident on the first wall is broadened considerably because of various interactions with the wall material and the blanket. The corresponding spectrum is shown in fig. 1 [10] and compared with those of

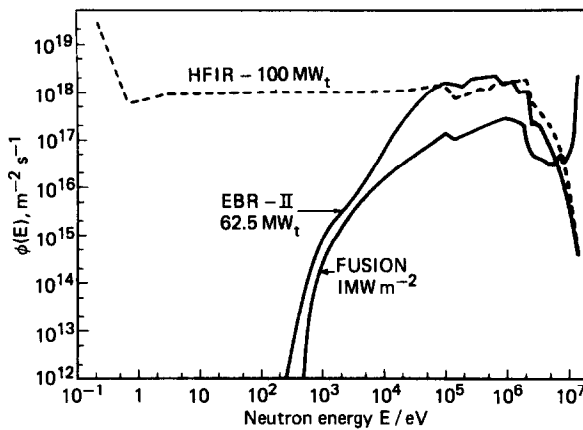


Fig. 1. Comparison of a fusion spectrum (1 MW m<sup>-2</sup> wall loading, stainless steel blanket) with neutron spectra in two experimental facilities (HFIR: High Flux Isotope Reactor, ORNL; EBR-II: Experiments Fast Breeder Reactor, Idaho Falls) [10].

two existing fission reactors. If we restrict ourselves to neutron energies which are needed to transfer sufficient energy for a significant amount of atoms to be displaced ( $> 0.1$  MeV), the similarity of the spectra up to energies of about 5 MeV is obvious. The situation is still more favourable at the magnet location because of additional slowing-down processes in the magnet shield. A comparison of the neutron spectrum produced in a research reactor with a typical fusion spectrum at the magnet location is shown in fig. 2 [11]. It will be noted that only

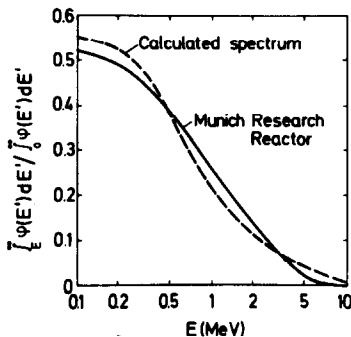


Fig. 2. Integrated neutron flux spectrum normalized by the total flux for the magnet location in a fusion reactor compared with the fission spectrum of the low temperature irradiation facility at FRM, Munich [11].

about 5% of the neutrons have energies greater than 4 MeV. However, because of the large damage energies of these neutrons, irradiation experiments in fission reactors should be supplemented by high-energy neutron irradiations in order to obtain reliable results.

Concerning the neutron flux integrated over all energies greater than 0.1 or 1 MeV, respectively, and over the total lifetime of the magnet, i.e. the neutron fluence, it is generally agreed [11] that the shielding should be designed to limit the fluence to  $4 \times 10^{22}$  m<sup>-2</sup> ( $E > 0.1$  MeV) or  $\sim 2 \times 10^{22}$  m<sup>-2</sup> ( $E > 1$  MeV). However, because the shielding may be difficult and less effective at certain positions of the magnet (development of a "hot spot") irradiation experiments should be performed into the  $10^{23}$  m<sup>-2</sup> fluence range.

The processes of damage production by fast neutrons are as follows: first, the incident particle transfers energy to a lattice atom by elastic or inelastic reactions (the latter become important for neutron energies  $\geq 2$  MeV only). Second, the primary knock-on atom distributes its energy to the neighbouring lattice atoms until it is no longer able to produce further atomic displacements. Finally, some energy is dissipated in this displacement cascade eliminating some unstable Frenkel pair configurations. The total time involved in this process is of the order of  $10^{-11}$  s and the size of the cascades is in the range from 5–20 nm. If the sample is kept at sufficiently low temperatures, the configuration of vacancies and interstitials is stable; at higher temperatures the defects may become thermally activated and mobile and may undergo rearrangement and annihilation processes leading to local clusters of point defects. Consequently, the temperature maintained during irradiation is an important parameter and should be as close as possible to the operating temperature of the fusion magnet. Unfortunately, there are very few irradiation facilities available which allow these stringent conditions to be met.

There is some experimental evidence that the irradiation temperature is less important in the case of A15 superconductors, where the damage of the long-range ordered structure seems to be the primary reason for the changes of the superconducting properties. For NbTi, on the other hand, the structure of defects produced by the irradiation and its interaction with the metallurgical microstructure present prior to irradiation determine the response of the superconductor. Hence, it is necessary to investigate the flux-pinning mechanisms in NbTi in some detail. Furthermore, it is expected that the temperature maintained during irradiation is a more critical parameter than in the A15's, as will shown in section 4.

### 3. Flux-pinning in NbTi

The general properties of the alloy system Nb–Ti have been reviewed recently [12–14]. Materials suitable for commercial applications because of their  $T_c$  and  $H_{c2}$  values are found in the range from 40 to ~55 wt% Ti. Of course, the main interest of all the different manufacturers lies in the optimization of critical current densities, which, in general, involves sophisticated multiple thermomechanical treatments whose particular effects on the metallurgical microstructure are largely unknown. Recent efforts to investigate the metallurgical state of conductors which are actually used in present large-scale applications are, therefore, extremely valuable [15,16].

Earlier work on conductors subjected to much simpler thermomechanical treatments has provided a lot of insight into the pinning action of different microstructural properties [17–23], although the onset and contribution of normal conducting  $\alpha$ -Ti precipitates on the niobium-rich side of the phase diagram is still not completely clear. A summary of the present understanding of flux pinning in the interesting range of Ti concentration may be given as follows.

According to Hillman [17–19], a precipitation of the  $\alpha$ -phase can be practically excluded for Ti concentrations below 45 (maybe 42) wt% Ti. Hence, flux pinning

in these materials is caused by the defect structure introduced by the initial severe cold-work and is based on interactions of the flux lines with dislocations and dislocation cells (sub-band structure). According to [20,21], a subsequent heat treatment has a significant effect on the bulk-pinning forces,  $P_V = B \times j_c$ , which is caused by different processes depending on the annealing temperature. At low annealing temperatures (300–385°C) the size of the cells increases slowly and varies between 20 and 50 nm depending on the starting conditions induced by the initial cold-work (sub-bands). However, in this temperature range a drastic increase of the pinning force is observed, which is related to the migration of dislocations into the cell walls and, hence, an increase of the elementary pinning forces, presumably through the  $\Delta\kappa$  effect ([24,25], cf. also section 4.5). Above this temperature, where most of the dislocations have been removed from the interior of the cells, the cells start to grow fairly rapidly and reach a size of ~400 nm at an annealing temperature of 600°C. In this temperature range a continuous decrease of  $j_c$  is observed, which follows a  $1/(\text{cell size})$  behaviour (cf. the solid line of fig. 3 obtained for Nb–44 wt% Ti [20]).

If the annealed samples are subjected to a final cold-working, the change of the cell size will again influence the magnitude of the bulk pinning force. However, whether an increase or a decrease of  $j_c$  is

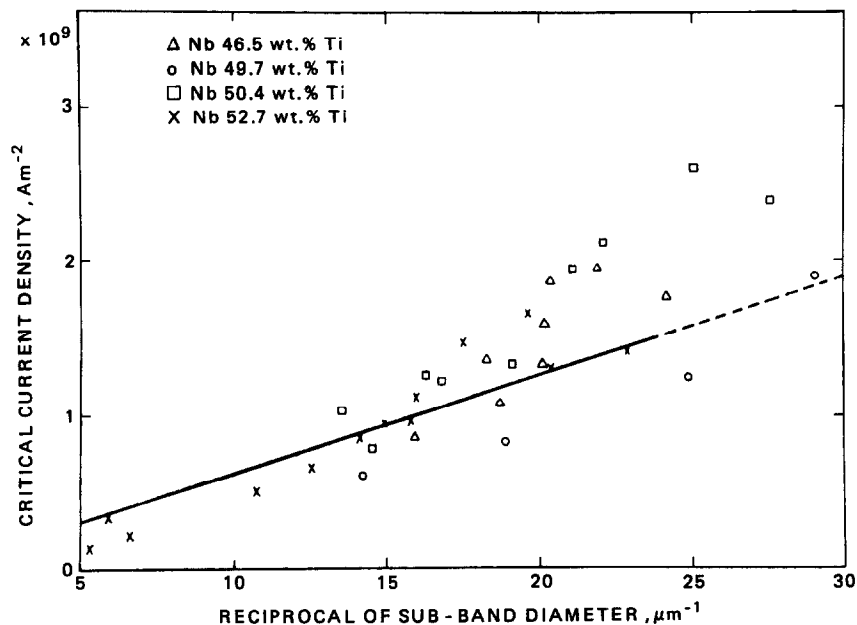


Fig. 3. Dependence of the critical current density on the inverse cell size (solid line: [20], data points: [15]) [15].

observed depends on the initial annealing temperature. For materials which were annealed below the optimum temperature of about 385°C, a decrease of  $P_V$  is expected, whereas all other materials should exhibit an increase of  $P_V$ .

A different situation exists in samples with higher Ti concentrations, where flux pinning by normal conducting  $\alpha$ -Ti precipitates prevails. Because of their larger elementary pinning force the precipitates provide the major contribution to  $P_V$ ; the rest is contributed again by the mechanisms mentioned above. According to [17,18], the precipitates are nucleated preferentially along the initial sub-band structure. Therefore, the initial degree of cold-work and the subsequent low temperature ( $< 400^\circ\text{C}$ ) annealing time will be essential for the

precipitation process. However, because of the significant texture of this structure and the corresponding anisotropy of the precipitate arrangement, only a small number of precipitates will contribute to  $P_V$ . In the course of subsequent cold-working the distribution of precipitates becomes increasingly homogenous leading to an increase of active pinning centres and, consequently, to a rapid increase of  $P_V$ . This trend is reversed only at extremely high degrees of cold-working, where again an anisotropic distribution of precipitates is established. In fact, deviations from the  $1/(\text{cell size})$  dependence of the critical current density were recently related to the appearance of  $\alpha$ -precipitates [15] (cf. the symbols in fig. 3). This understanding of the flux-pinning processes was essentially confirmed by a recent

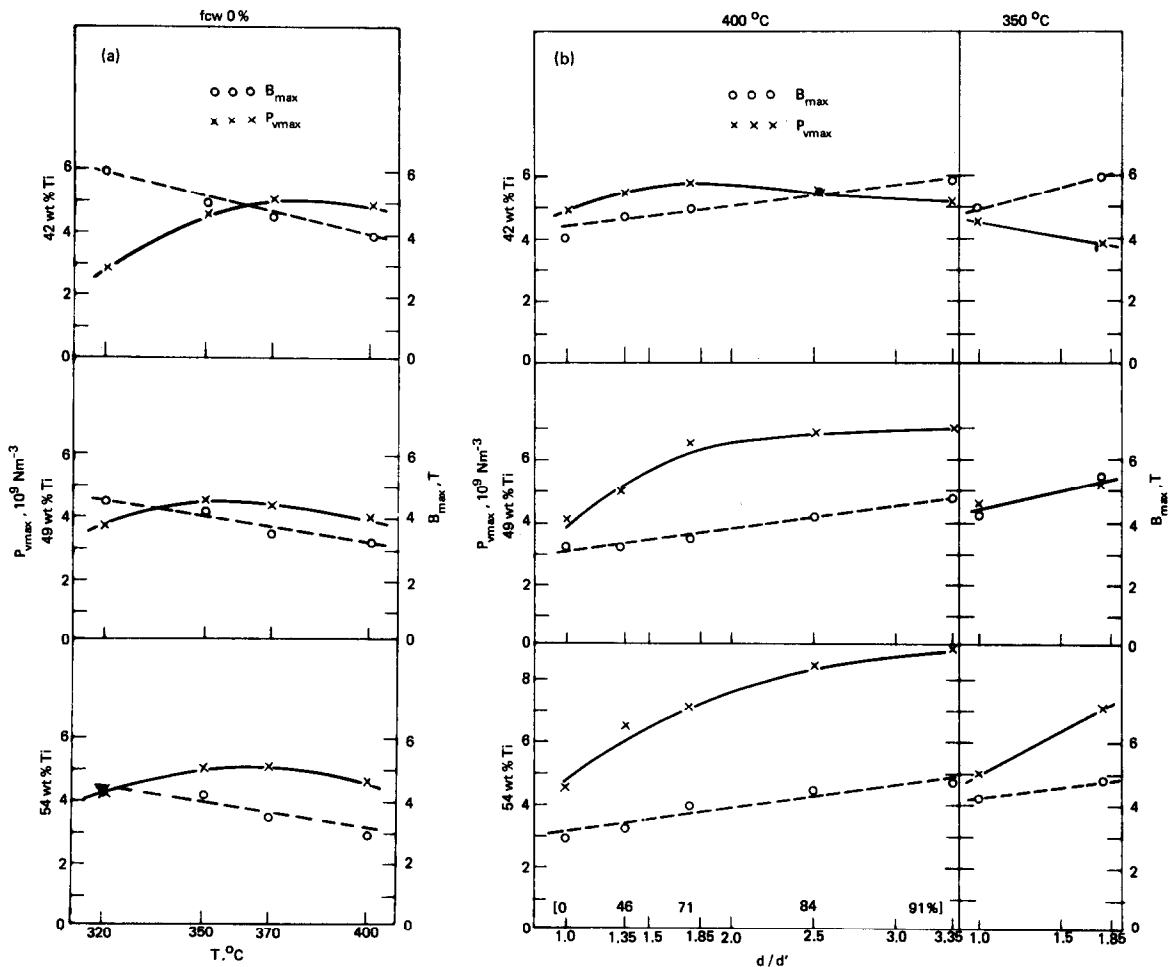


Fig. 4. Maximum pinning forces  $P_{V \max}$  (xxx and solid lines) and magnetic field  $B_{\max} = B(P_{V \max})$  (ooo and broken lines) versus the metallurgical variation parameters [27].  $d/d'$  is the ratio of wire diameters prior to and after final cold work.

comprehensive study of fairly simple NbTi systems differing in their Ti concentration and final thermomechanical treatment [26,27]. The results on these single-core conductors are shown in fig. 4, where the maxima of the pinning curves are plotted versus one metallurgical variation parameter (e.g. the annealing temperature), whereas the other parameter (e.g. the final cold-working) is kept constant. The samples containing 42 wt% Ti initially show a drastic increase of  $P_{V \max}$  with increasing annealing temperature (solid lines in fig. 4), a maximum near 380°C, and a decreasing tendency towards higher temperatures. The increase of  $P_{V \max}$  between 320 and 380°C amounts to about 85%. Cold-working following an annealing treatment at 400°C results in an initial increase by about 20% and a subsequent reduction of  $P_{V \max}$ ; the same treatment following an anneal at 350°C immediately results in a decrease of  $P_{V \max}$ . The dominating influence of annealing at low temperatures, and the further response to the thermomechanical treatment, emphasize the role of dislocation and cell pinning in these materials.

In contrast to this, the samples containing 49 and 54 wt% Ti show only small influences of the initial annealing temperature and a maximum increase of  $P_{V \max}$  by about 20%. The final cold-working which was related to a more efficient arrangement of the precipitates does, however, lead to a significant increase of  $P_{V \max}$  of the order of 100% which is independent of the preceding annealing temperature. This behaviour, which is in contrast to the result on Nb-42 wt% Ti, demonstrates the minor contribution of cell pinning and the dominance of precipitate pinning in the cold-worked samples.

In summary, considering the defects produced by neutron irradiation and their interaction with these two types of pinning mechanisms we have to expect significantly different responses of the critical current densities upon irradiation. Unfortunately, however, in most cases the sample characterization prior to irradiation is not too accurate as will be shown in the following sections.

## 4. Results of neutrons irradiation

### 4.1. Transition temperature

As expected from earlier work on elemental superconductors, in particular Nb, radiation-induced changes of  $T_c$  are insignificant in NbTi alloys. Under various conditions, i.e. low and ambient temperature neutron irradiation, up to fluences of  $\sim 10^{23} \text{ m}^{-2}$  ( $E > 1 \text{ MeV}$ ) decreases of  $T_c$  by about 0.15 K were found for different

alloy compositions (e.g. [27]). Also 25 MeV oxygen ( $3.6 \times 10^{20} \text{ m}^{-2}$ ) [28] or 15 MeV deuteron irradiation ( $1 \times 10^{21} \text{ m}^{-2}$ ) [29] carried out at low temperatures produced changes in  $T_c$  of this magnitude. Only two exceptions were reported [6,30], which were obtained under completely different experimental conditions and showed a decrease of  $T_c$  by 0.6 K. Whereas the ambient temperature irradiation result [30] for one particular sample of Nb-45 wt% Ti is inconsistent with other work, the second one obtained on samples of nominally the same composition [6] after low temperature 14 MeV neutron irradiation up to about  $8 \times 10^{20} \text{ m}^{-2}$  should be checked by another experiment, since an influence of the greatly enhanced damage energy is expected only on the critical current densities (cf. below). In any case, the changes of  $T_c$  are very small and may be neglected. Concerning the upper critical field  $H_{c2}$ , there are very few experiments available [29,31], which also indicate only small changes of this quantity. Certainly, a more detailed investigation of radiation effects on  $H_{c2}$  would be desirable.

### 4.2. Critical current densities: ambient temperature irradiation

If we recall the nature of defects mentioned in section 2, which are produced during ambient temperature (60–100°C) irradiation, it follows immediately that these results are applicable to fusion magnet considerations only with certain restrictions. However, experiments of this type are considerably less costly than low temperature irradiation, provide more space for samples to be

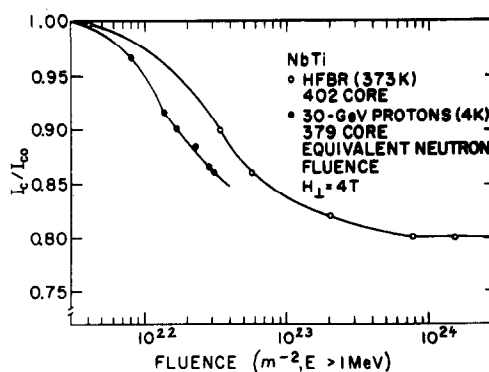


Fig. 5. Change of critical currents in Nb-45 wt%Ti multifilamentary wires. ○○○ neutron irradiation (402 core conductor at 100°C), ... 30 GeV proton irradiation (379 core conductor at 4.2 K). All measurements refer to 4.2 K and a magnetic field of 4 T [33].

irradiated simultaneously and can be extended to high fluences more easily. A summary of the work published until 1977 has been tabulated by Sekula [32], further work is found in [27] and [33].

The samples investigated vary in their Ti concentration between 36 and 54 wt% and comprise single-core and multifilamentary wires. Two aspects of these results shall be discussed briefly: (1) the response of  $j_c$  to very high neutron fluences ( $1.4 \times 10^{24} \text{ m}^{-2}$ ,  $E > 1 \text{ MeV}$ ), and (2) the influence of the metallurgical sample conditions prior to irradiation on the subsequent irradiation-induced changes of  $j_c$ .

The results of high-fluence neutron irradiation of a commercial multifilamentary Nb-45 wt% Ti conductor are shown in fig. 5 [33]. The interesting feature of this graph is the obvious tendency of the  $j_c$  ratio to saturate at high fluences ( $\geq 8 \times 10^{23} \text{ m}^{-2}$ ,  $E > 1 \text{ MeV}$ ) at a level of 0.80, i.e. the maximum reduction of the critical current amounts to 20%. Because of the similarity with the commonly observed resistivity saturation at high fluences [34,35] the authors suggest that the normal-state resistivity saturation in NbTi is responsible for the decrease of the pinning forces (cf. section 4.5). For the purpose of comparison the results obtained on a similar

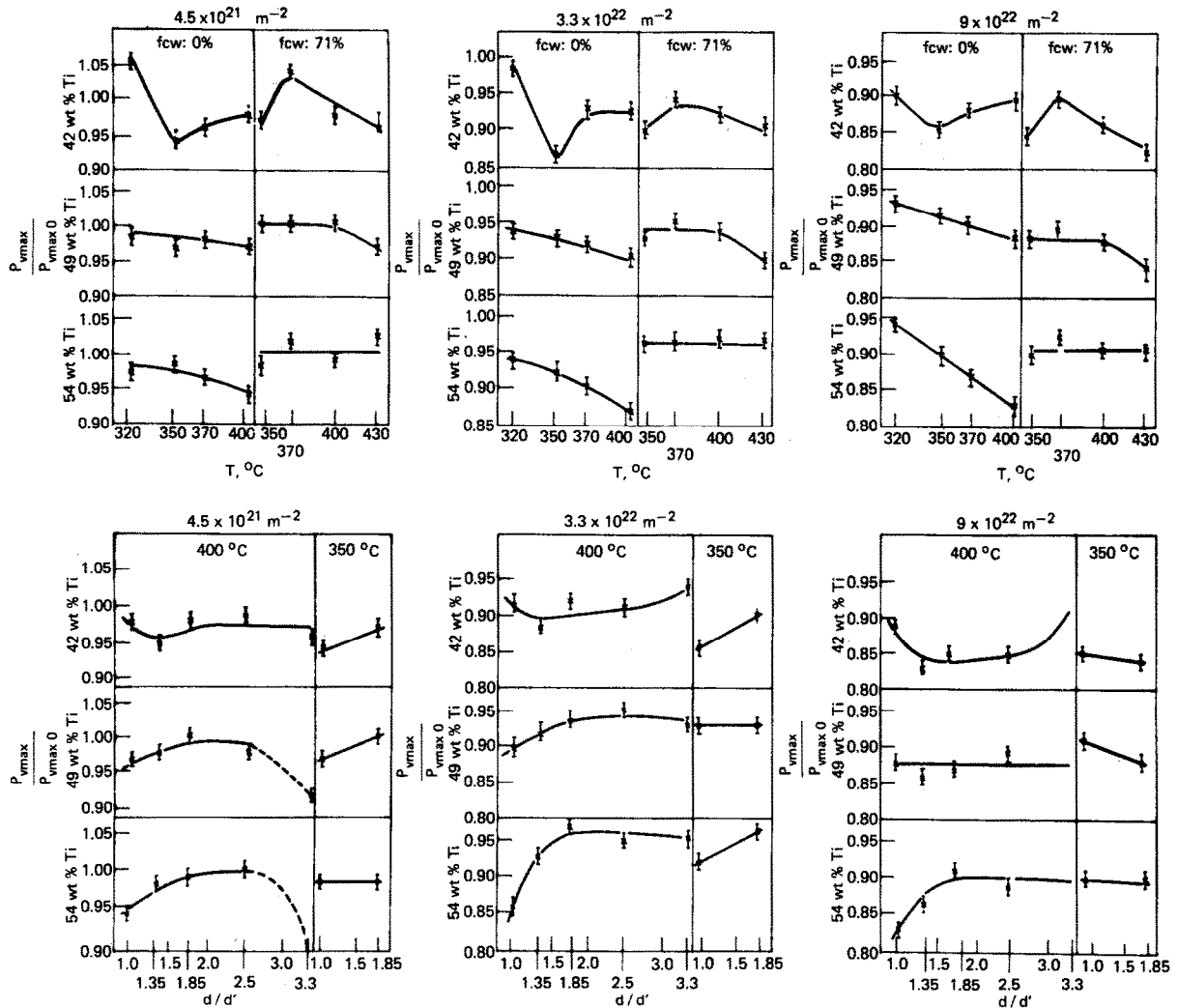


Fig. 6. Normalized maximum pinning forces plotted versus the metallurgical variation parameters at three neutron fluences:  $4.5 \times 10^{21}$ ,  $3.3 \times 10^{22}$ ,  $9 \times 10^{22} \text{ m}^{-2}$  ( $E > 1 \text{ MeV}$ ). (a) Influence of annealing temperatures at 0% and 71% final cold-working, respectively. (b) Influence of final cold-working conditions for annealing temperatures of 400 and 350 °C, respectively [27].

sample, which was subjected to 30 GeV proton irradiation at 4.2 K, are included in fig. 5 and shown as a function of "equivalent" neutron fluence, which is calculated on the basis of the damage energy concept (e.g. [36–38]). It is interesting to note that low temperature irradiation leads to a similar, but faster, decrease of the critical currents, which is again in agreement with previous observations of resistivity changes upon irradiation at different temperatures. From the trend of the data a saturation effect can be expected.

Similar conclusions were arrived at in the second work to be discussed [27], where a completely different approach was used. In this study a broad spectrum of well characterized single-core conductors differing in their Ti content and thermomechanical treatment were irradiated simultaneously in order to investigate the interaction of radiation-induced defects with different pinning structures (cf. also section 3 and fig. 4). The results are shown in fig. 6, where the maximum of the pinning forces normalized to the corresponding value prior to irradiation is plotted versus the metallurgical variation parameters for three different neutron fluences. Fig. 6(a) shows the influence of the annealing temperature for 0% and 71% final cold-working, respectively. Considering again the samples which have not undergone a final cold-working, significant and non-systematic effects of the annealing temperature on the change of  $P_{V \max}$  are observed at 42 wt% Ti, whereas smaller and continuous effects prevail in samples with 49 and 54

wt% Ti, respectively. On the contrary, the cold-worked state samples with 54 wt% do not show any influence of the annealing temperature, samples with 49 wt% show only a small effect at 430°C, and samples with 42 wt% again show significant and unsystematic changes. The influence of cold-working at constant annealing temperature is shown in fig. 6(b). It should be noted that the changes of  $P_{V \max}$  are smallest in severely cold-worked samples of 49 and 54 wt% Ti and are significant again in all samples containing 42 wt% Ti. The remaining and comparatively small decreases of the pinning forces in the Ti-rich materials are obviously caused by the reduction or removal of the cell pinning contribution.

There are two conclusion to be drawn from these data: Firstly, materials with *predominant precipitate pinning* are affected least by irradiation and a comparatively broad variation of the initial metallurgical treatments leads roughly to the same changes of  $j_c$ . Secondly, the rather simple rule that materials with higher initial critical current densities  $j_{c0}$  always show larger  $j_c$  degradations than those with lower  $j_{c0}$  does not hold in this simple form. This is demonstrated in fig. 7, where the changes of  $j_c$  at a given neutron fluence ( $2.25 \times 10^{22} \text{ m}^{-2}$ ,  $E > 1 \text{ MeV}$ ) and for a fixed field of 5 T are plotted versus  $j_{c0}$ . The variation in the 42 wt% Ti series is completely irregular and emphasizes again the role of cell size and density. Similar unsystematic changes occur in the low- $j_{c0}$  samples of the other materials, whereas the *higher- $j_{c0}$*  samples with predominant precipitate pin-

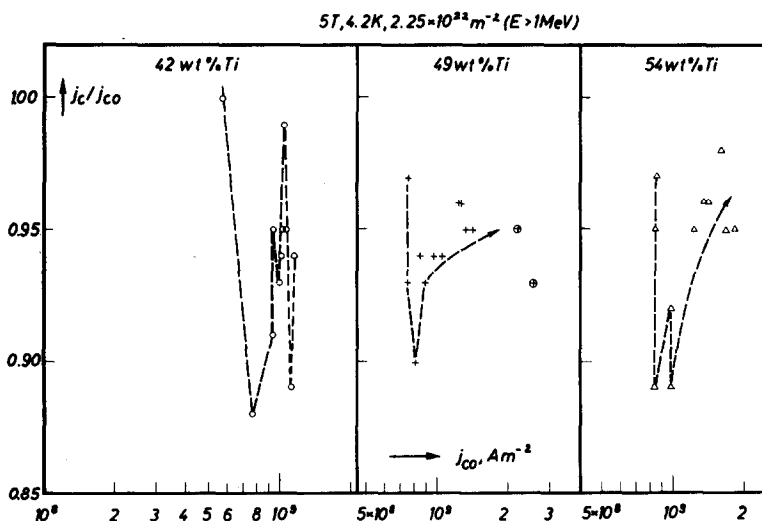


Fig. 7.  $j_c/j_{c0}$  plotted versus  $j_{c0}$  for a broad spectrum of NbTi conductors. The data refer to a fluence of  $2.25 \times 10^{22} \text{ m}^{-2}$  ( $E > 1 \text{ MeV}$ ) and were taken at  $T = 4.21 \text{ K}$  and  $B = 5 \text{ T}$ .

ning tend to show *smaller*  $j_c$  degradations. Two further observations of this study should be mentioned. First, in all the cold-worked samples, i.e. those with a reasonable defect structure, the changes of  $j_c$  are field independent in the field range investigated (usually 2–6 T). Second, from a comparison of the  $j_c$  dependence on neutron fluence for high  $j_c$  conductors ( $> 1.3 \times 10^9 \text{ A m}^{-2}$  at 5 T) the irradiation-induced degradation is smaller than the improvement of  $j_c$  which can be achieved by an optimized metallurgical treatment prior to irradiation.

#### 4.3. Critical current densities: low temperature irradiation and annealing

Low temperature reactor neutron irradiation ( $T_{\text{irr}} = 4.2\text{--}6 \text{ K}$ ) of NbTi were made at the Munich, Argonne and JAERI facilities, 27 and 77 K irradiations in Grenoble and, more recently, 77 K irradiations in Vienna. A summary of this work, which refers to a few different conductors in the range 33–54 wt% Ti, can be found again in the review by Sekula [32], further work in [39–41]. Recently, the first results of neutron irradiation at 4.2 K using monoenergetic 14.8 MeV neutrons were reported [6].

As an example, we show the results on a series of Nb–50 wt%Ti multifilamentary conductors obtained by Söll et al. [42] in fig. 8. The pinning forces measured prior to irradiation confirm again the role of cell and precipitate pinning, respectively, by the drastic decreases upon high temperature anneals as well as the significant increase with the formation of precipitates (fig. 8(a)). The irradiation data show some features, which are in common with the results discussed in the previous section. First, the changes of  $j_c$  are again found to be field independent in the field range investigated (0–5 T). Second, the radiation-induced decrease of  $j_c$  is considerably smaller in the sample with precipitate pinning. A tremendous increase of  $j_c$  is observed in the worst conductor, which demonstrates the pinning capability of the defect cascades in NbTi produced at this low temperature.

First results of low temperature 14 MeV irradiation of Nb–45 wt% Ti were reported recently [6] and compared with fission reactor irradiations of a similar multifilamentary sample [39]. In both cases  $j_c$  degradations of about 3% were observed at 4 T, but for fluences of  $5 \times 10^{21} \text{ m}^{-2}$  ( $E > 0.1 \text{ MeV}$ ) and  $7 \times 10^{20} \text{ m}^{-2}$  ( $E = 14.8 \text{ MeV}$ ), respectively. If we use again the concept of damage energies and calculate these damage energies in Nb for 14 MeV neutrons (256 keV barns) and the Argonne spectrum (55.7 keV barns), respectively, [43], the scaling of the above fluences for the same change of

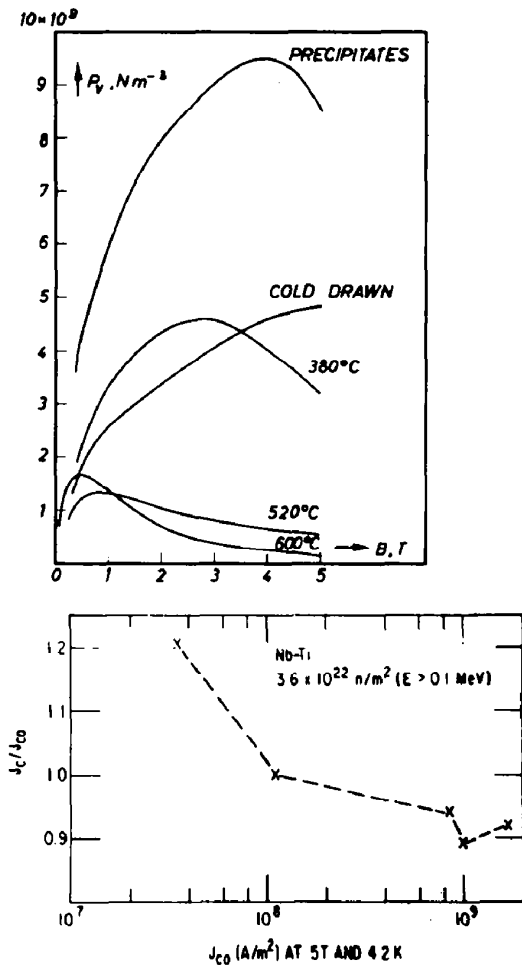


Fig. 8. Low temperature neutron irradiation of Nb–50 wt% Ti. (a) Bulk pinning curves prior to irradiation. (b) Change of critical current densities after irradiation to a fluence of  $3.6 \times 10^{22} \text{ m}^{-2}$  ( $E > 0.1 \text{ MeV}$ ) versus the initial critical current density  $j_{c0}$  at 5 T (after [42]).

$j_c$  is within the experimental error. An extension of these comparisons to higher fluences and magnetic fields would certainly be most valuable.

Important information on the flux-pinning mechanisms is obtained from the annealing behaviour following low temperature irradiation. A summary of results obtained on not too well characterized multifilamentary samples of Nb–50 wt%Ti is shown in fig. 9 [44]. Three of the samples (Nos. 2–4) were exposed to a neutron fluence of  $4.5 \times 10^{22} \text{ m}^{-2}$  ( $E > 0.1 \text{ MeV}$ ) at 5 K and subsequently annealed for 5 min at 60, 100, 200 and 270 K, respectively; sample 1 was irradiated to  $7.5 \times$



$10^{22} \text{ m}^{-2}$  and shows the highest  $j_c$  degradation ever reported for NbTi. The influence of annealing is as follows: after an initial temperature range (5–60 K), where no recovery occurs, two major steps are observed in the temperature intervals 60–100 K and 100–200 K followed by a small additional effect up to room temperature. The residual  $j_c$  degradation varies between 0 and 5%. The more severely damaged sample No. 1 shows also a considerable recovery effect, the remaining  $j_c$  degradation, however, is close to 20%.

This temperature dependence may be related directly to the mechanisms of flux pinning and their irradiation-induced changes (cf. section 4.5): whereas low temperature irradiation produces stable defects, which increase the resistivity of the material mainly within the dislocation cells and thereby reduce their pinning action, the following anneal provides thermal energy for the defects to become mobile and eventually recombine. As the defects recover, the resistivity decreases again and the pinning force increases. This was demonstrated most clearly by direct resistivity measurements on Nb–48 wt% Ti [34]: low temperature irradiation to a fluence of  $1.8 \times 10^{22} \text{ m}^{-2}$  ( $E > 0.1 \text{ MeV}$ ) produced a change of resistivity by 40%. At 100 and 290 K, 40 and 70% of the total change were found to have recovered, in close agreement with the corresponding recovery of the critical currents.

The results shown in fig. 9 are also valuable for determining the role of irradiations carried out at higher temperatures, e.g. at 27 and 77 K [40,41,45]. It will be noted that liquid nitrogen temperature is just in the first half of the first recovery step. The changes of  $j_c$  compared with 4 K irradiation amount to  $\sim 2\%$ . The same

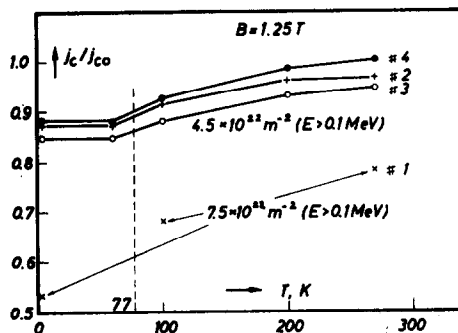


Fig. 9. Recovery of  $j_c/j_{c0}$  up to room temperature for 4 different samples of Nb–50 wt% Ti (measured at 4.2 K and 1.25 T), after [44]. The measurements were made on one filament (Nos. 1–3:  $11 \mu\text{m}$  filament diameter, No. 4:  $21 \mu\text{m}$ ) of multifilamentary wires.

result was obtained by Couach et al. [45], who directly compared 27 and 77 K irradiations on a commercial multifilamentary wire. Bearing these limitations in mind, less costly irradiation experiments at liquid nitrogen temperature can be used for special purposes, e.g. the simultaneous irradiation of a larger number of samples.

#### 4.4. Critical current densities: low temperature irradiation and thermal cycles

Not much work on the systematic inclusion of room temperature anneals after each low temperature irradiation step has been reported so far, although this process is certainly the most important one for fusion magnet considerations. As an example the results for proton irradiation of a Nb–45 wt% Ti multifilamentary conductor [33] are shown in fig. 10. The dashed line refers to data taken entirely at low temperatures and a final room temperature anneal, which results in 50% recovery of the  $j_c$  degradation. The second run, which included a thermal cycle at roughly half of the total fluence, shows a comparable amount of recovery at the low fluence value, smaller  $j_c$  degradations in the course of the following irradiation and again comparable final recovery effects. The final values of  $j_c/j_{c0}$  are 0.86, 0.92 and 0.94 for pure low temperature irradiation and with one or two annealing cycles, respectively. A more complete set of data was obtained recently [41] for a series of different NbTi conductors, which were irradiated at 77 K and cycled to room temperature after each irradiation step.

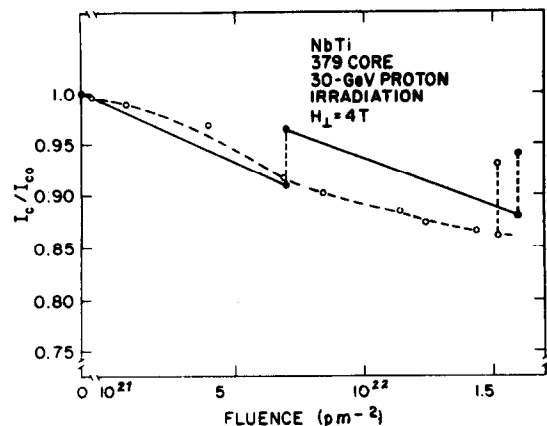


Fig. 10. Changes of critical currents measured at 4 T with proton fluence (Nb–45 wt% Ti, 379 core conductor). O O irradiation at 4.2 K, final anneal at room temperature; ... irradiation at 4.2 K, one intermediate and one final anneal to room temperature [33].

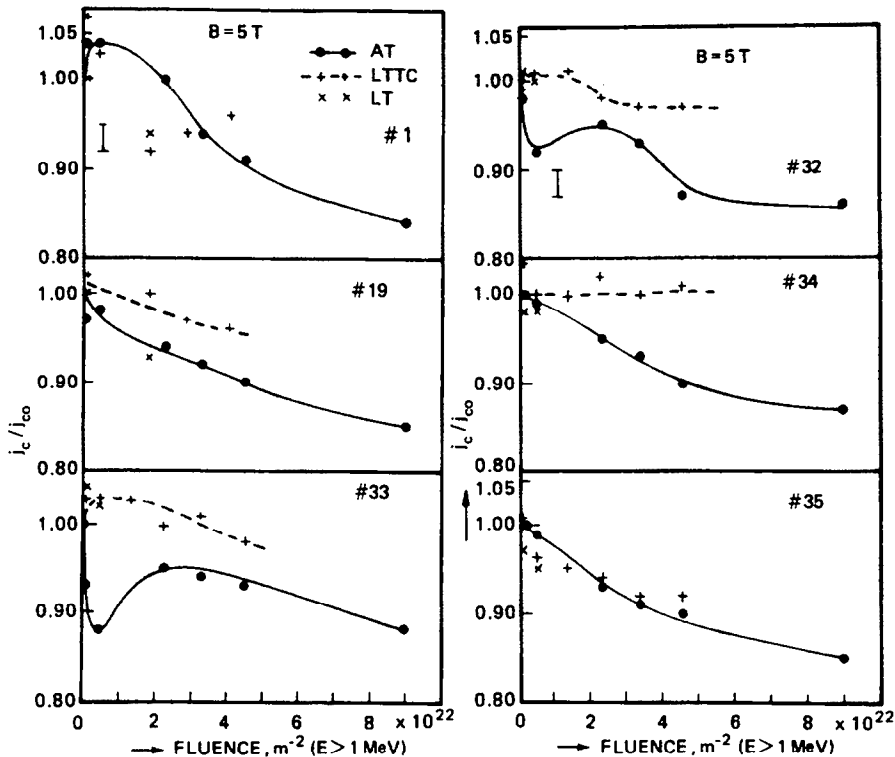


Fig. 11. Changes of critical current densities measured at 5 T with fast neutron fluence. AT, LT: irradiation at ambient temperature and 77 K, respectively; LTTC: irradiation at 77 K and thermal cycle to room temperature. No. 1: Nb-42 wt% Ti, lowest  $j_{c0}$ ; Nos. 19, 32, 33: Nb-42, 49, 54 wt%Ti, highest  $j_{c0}$  of each series; Nos. 34, 35: Nb-49 wt%Ti, Multifilamentary conductors [41].

The results are shown in fig. 11 and compared with the ambient temperature irradiation of the same samples, which was discussed in section 4.2, and some preliminary data on 77 K irradiation without the thermal cycle. The most significant result is the almost complete recovery in samples no. 19 and 32-34, where the overall changes of  $j_c$  are smaller than 4% up to fluences of  $\sim 5 \times 10^{22} \text{ m}^{-2}$  ( $E > 1 \text{ MeV}$ ). On the other hand Nos. 1 and 35 show changes of  $j_c$  which are similar to the ambient temperature result.

An explanation of this differing response is not yet supported by experimental evidence. However, one feature which is common to each of these two groups of samples is the final treatment prior to irradiation: samples No. 1 and 35 were subjected to a final anneal, whereas the other samples were cold-worked as the final preparation step. In the course of the previous ambient temperature irradiation work [27] residual resistivity measurements as a function of neutron fluence were made, which showed no changes in the cold-worked

samples ( $\text{RRR} \sim 45$ ), but a degradation by a factor of two ( $\text{RRR } 97 \rightarrow 53$ ) in the annealed materials. Therefore, the change of stabilizer performance could play an important role in explaining these differences, in particular in the multifilamentary wire. Direct measurements on the influence of stabilizer resistivity on the voltage-current characteristic were reported, e.g. by Söll et al. [42]. More information on the response of different stabilizing materials to neutron irradiation, which certainly deserves still more attention, can be found, e.g., in [5].

#### 4.5. Discussion of results in terms of flux-pinning mechanisms

The bulk of the experimental evidence presented in the last sections, in particular experiments on those materials containing additional contributions of precipitate pinning, demonstrates most clearly that the primary source of radiation effects is the change of

dislocation cell pinning. The current understanding of the physics involved may be summarized as follows.

The pinning action of a dislocation cell results from the significantly different physical properties of the cell wall and the interior of the cell [24,25]. Because of the highly increased dislocation density within the wall the normal-state resistivity  $\rho_n$  and, hence, the Ginzburg-Landau parameter  $\kappa$  are strongly enhanced compared with the cell core (fig. 12). This local variation of  $\kappa$  results in variations of the free energy and, hence, a bulk pinning force, which is proportional to  $\Delta\kappa$ . The influence of neutron irradiation as well as the subsequent annealing behaviour may be understood well on the basis of this pinning mechanism [44]. Consider first optimized NbTi conductors, i.e. materials with a high

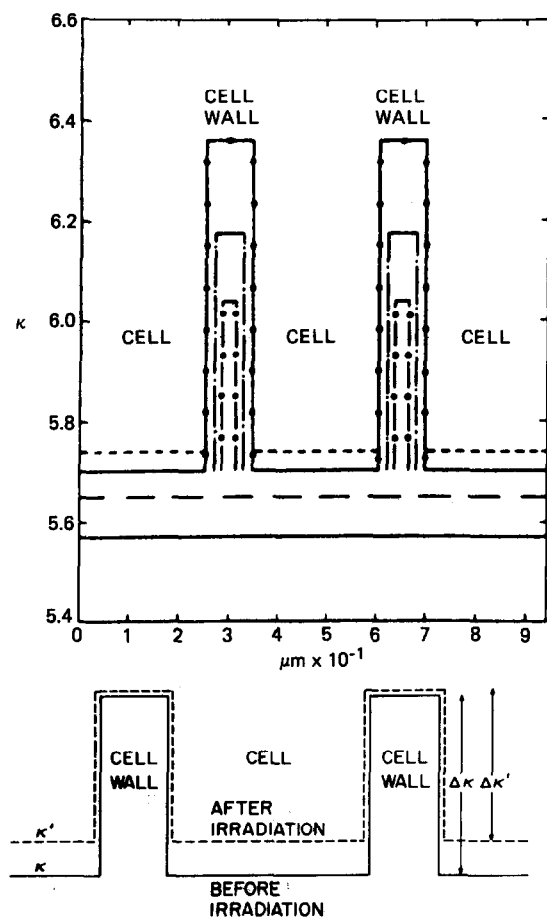


Fig. 12. Effect of increasing cold-work on the Ginzburg-Landau parameters within the cell walls and cores, respectively (a); effect of irradiation on the same parameters (b).

density of sufficiently small cells. In this case, the radiation-induced defects will concentrate within the cell cores, whereas the high concentration of dislocations and associated strain fields within the walls will lead to enhanced annihilation of Frenkel pairs. To first order, the change of resistivity and, hence, Ginzburg-Landau parameter  $\kappa$  within the walls can be neglected entirely (fig. 12). Therefore, the net effect is a reduction of  $\Delta\kappa$  and the pinning force. Now, if the irradiated sample is subjected to an annealing treatment, the thermal energy increases the mobility of defects, which migrate toward the walls, where they can be trapped, or annihilate. This process, which is, of course, strongly temperature dependent, will again decrease the resistivity within the cell cores and lead to a (partial) recovery of the original pinning forces. In summary, this mechanism is well suited to explain the behaviour of metallurgically optimized (high  $j_{c0}$ ) conductors. In addition, the better performance of materials with predominant precipitate pinning can be understood by assuming that only the cell pinning contribution is affected in the way described, whereas precipitate pinning is essentially unaffected.

Concerning materials with low initial critical current densities  $j_{c0}$ , i.e. with a low density and/or large sizes of the cells, the situation is much more involved. This is caused by the fact that displacement cascades produced during low temperature irradiation as well as defect clusters produced at ambient temperatures can act as additional pinning centres. Therefore, the interplay of this effect with the reduction of pinning forces through the  $\Delta\kappa$  effect as discussed above depends in the most sensitive way on the metallurgical state of the sample prior to irradiation and does not permit any general predictions.

In summary, it should be pointed out that, although flux pinning through the  $\Delta\kappa$  effect seems to provide an adequate description of the observed behaviour, alternative mechanisms similar, e.g., to the enhancement of scattering at grain boundaries [46] are feasible. Therefore, additional work on bulk pinning forces, which should be extended up to the critical field  $H_{c2}$ , in conjunction with electron-microscopic investigations of the defect structure is still desirable.

## 5. Conclusions

From the work reported so far, which was presented in the last sections, a fairly consistent picture of radiation-induced effects in the alloy superconductor NbTi has emerged. (No reference has been made to the other

alloys investigated previously, e.g. NbTa [47] and NbZr [29], because they are of no interest for present-day applications.) The following summary of this information will enable specific question to be asked which should be answered by future experiments. The experimental evidence is as follows:

(1) The decrease of transition temperature  $T_c$  with neutron fluence is very small (0.15 K) and may be neglected for application considerations. The physical reason for this effect is not completely clear. It may be related to the removal of energy-gap anisotropy by the introduction of additional scattering centres as observed in many pure elemental superconductors (cf., e.g., [48]); on the other hand, in most cases the material is already in the "dirty" limit prior to irradiation, where this effect should have vanished.

(2) The response of NbTi to particle irradiation is essentially determined by the radiation-induced changes of the metallurgical microstructure, which is responsible for flux pinning and, hence, the critical current densities achievable.

(3) The changes of critical current densities observed under a variety of conditions can be explained consistently by assuming that the defects produced by the irradiation affect the pinning strength of the dislocation cells. The mechanism involved is the increase of normal state resistivity within the cell cores compared with the cell walls, which decreases the difference of the Ginzburg-Landau parameters and, hence, the pinning force.

(4) Those materials with significant contributions of precipitate pinning show considerably smaller degradations of  $j_c$ . This is consistent with the conclusion mentioned above if it is assumed that the cell pinning contribution is affected in the normal way, but precipitate pinning is unaffected by the irradiation.

(5) With one exception all the results show that the degradation of  $j_c$  will not exceed 20%.

(6) Annealing to room temperature and, in particular, multiple thermal cycles lead to almost complete recovery of  $j_c$ . This again is consistent with the pinning mechanism based on the radiation-induced change of the normal-state resistivity.

(7) Most of the work performed on reasonably high- $j_{c0}$  superconductors shows that the changes of  $j_c$  are independent of magnetic fields in the range investigated (usually 0–6 T).

From the above list it is perfectly clear that the alloy superconductor NbTi will not be a critical component of a fusion magnet. However, it is necessary to bear in mind, first, that the data presented are mostly derived from experiments which do not fully represent the conditions to be expected for a fusion magnet and, second,

that differences of a few percent in the coil performance may lead to significant design changes. Therefore, the following questions should be asked, which can only be qualitatively answered today:

Should commercial materials be tailored to contain more precipitates? What is the  $j_c$  degradation of commercial NbTi superconductors at 8 T, which were exposed to low temperature (4.2 K) reactor neutron irradiation up to a fluence of  $\sim 10^{23} \text{ m}^{-2}$ ? What is the corresponding effect of lower fluence 14 MeV irradiation? For both of these irradiation conditions, what is the effect of multiple thermal cycles to room temperature? For all of these short sample measurements, what is the influence of stabilizer degradation? What are the effects of additional mechanical stress on all these data? And finally, considering the superior stress performance of NbTi, if the concept of using NbTaTi at 2 K for 12 T magnets proves promising, what is the radiation response of this material at 12 T?

## References

- [1] B.S. Brown, H.C. Freyhardt and T.H. Blewitt (Eds.): *Radiation Effects on Superconductivity* (North-Holland, Amsterdam, 1978).
- [2] A.R. Sweedler, C.L. Snead, Jr. and D.E. Cox, in: *Treatise on Materials Science and Technology*, Vol. 14: *Metallurgy of Superconducting Materials*, Eds. T. Luhman and D. Dew-Hudges, (Academic Press, New York, 1979) p. 349.
- [3] C.L. Snead, Jr. and T. Luhman, in: *the Fusion Power Reactor*, Vol. 2. *Materials*, Eds. J.R. Weir, Jr. and J.H. Gittus.
- [4] H. Ullmaier, *Proc. Conf. Radiation Effects and Tritium Technology in Fusion Reactors*, Gatlinburg, 1975, Vol. II, p. 403.
- [5] B.S. Brown, *J. Nucl. Mater.* 97 (1981) 1.
- [6] R.A. Van Konynenburg, M.W. Guinan and J.H. Kinney, UCID-18938, February 1981.
- [7] R.R. Coltman, Jr. and C.E. Klabunde, *J. Nucl. Mater.* (1982) (in press).
- [8] P. Müller, G. Wallner, W. Weck and F. Rullier-Albenque, *J. Nucl. Mater.* 108 & 109 (1982) (this issue) p. 585.
- [9] R. Meier-Hirmer and H. Küpfer, *J. Nucl. Mater.* 108 & 109 (1982) (this issue) 593.
- [10] G.L. Kulcinski, *Contemp. Phys.* 20 (1979) 417.
- [11] M. Söll, in: *Radiation Effects on Superconductivity*, Eds. B.S. Brown, H.C. Freyhardt and T.H. Blewitt (North-Holland, Amsterdam, 1978), p. 168.
- [12] A.D. McInturff, in: *Treatise on Materials Science and Technology*, Vol. 14: *Metallurgy of Superconducting Materials*, Eds. T. Luhman and D. Dew-Hudges (Academic Press, New York, 1979), p. 99.
- [13] D.C. Larbalestier, *Adv. Cryog. Engrg.* 26 (1980) 10.
- [14] D.C. Larbalestier, *IEEE Trans. Magn.* MAG-17 (1981) 1668.

- [15] A.W. West and D.C. Larbalestier, *Adv. Cryog. Engng.* 26 (1980) 471.
- [16] A.W. West and D.C. Larbalestier, *Adv. Cryog. Engng.* 28 (1982) (in press).
- [17] I. Pfeiffer H. Hillman, *Acta Met.* 16 (1968) 1429.
- [18] H. Hillman, *Siemens Forsch. Entw. Ber.* 3 (1974) 197.
- [19] H. Hillman and K.J. Best, *IEEE Trans. Magn.* MAG-13 (1977) 1568.
- [20] D.F. Neal, A.C. Barber, A. Woolcock and J.A.F. Gidley, *Acta Met.* 19 (1971) 143.
- [21] R.G. Hampshire and M.T. Taylor, *J. Phys.* F2 (1972) 89.
- [22] P.R. Critchlow, E. Gregory and B. Zeitlin, *Cryogenics* 11 (1971) 3.
- [23] G. Rondelli, E. Olzi and F. Gherardi, *Z. Metall.* 71 (1980) 461.
- [24] A.M. Campbell and J.E. Evetts: *Critical Currents in Superconductors* (Taylor & Francis, London, 1972).
- [25] D. Dew-Hughes and M.J. Witcomb, *Phil. Mag.* 26 (1972) 73.
- [26] R.K. Maix, Thesis, Technical University of Wien, 1974.
- [27] F. Nardai, H.W. Weber and R.K. Maix, *Cryogenics* 21 (1981) 223.
- [28] K. Schmelz, G. Ischenko, B. Besslein, A. Greiner, S. Klaumünzer, P.Müller and H. Neumüller, *Phys. Lett.* 55A (1975) 315.
- [29] H.T. Coffey, E.L. Keller, A. Patterson and S.H. Autler, *Phys. Rev.* 155 (1967) 355.
- [30] H. Tsubakihara, T. Okada, T. Suita, T. Horiuchi, K. Matsumoto and S. Tsurutani, *J. Nucl. Sci. Technol.* 11 (1974) 452.
- [31] K. Wohlleben, *J. Low Temp. Phys.* 13 (1973) 269.
- [32] S.T. Sekula, in: *Radiation Effects on Superconductivity*, Eds. B.S. Brown, H.C. Freyhardt and T.H. Blewitt (North-Holland, Amsterdam, 1978) p. 91.
- [33] C.L. Snead, Jr., L. Nicolosi and W. Tremel, *Appl. Phys. Lett.* 31 (1977) 130.
- [34] B.S. Brown, T.H. Blewitt, T.L. Scott and A.C. Klank, *J. Nucl. Mater.* 52 (1974) 215.
- [35] A. Sosin and W. Bauer, in: *Studies on Radiation Effects in Solids*, Ed. G.J. Dienes, (Gordon and Breach, New York, 1969) Vol. 3, p. 153.
- [36] D.M. Parkin and C.L. Snead, Jr., *Proc. Int. Conf. on Fundamental Aspects of Radiation Damage in Metals*, Eds. M.T. Robinson and F.W. Young, Jr., CONF-751006 (1975) 1162.
- [37] M. Söll, K. Böning and H. Bauer, *J. Low Temp. Phys.* 24 (1976) 631.
- [38] M. Söll, in: *Radiation Effects on Superconductivity*, Eds. B.S. Brown, H.C. Freyhardt and T.H. Blewitt (North-Holland, Amsterdam, 1978) p. 122.
- [39] R.C. Birtcher, B.S. Brown and T.L. Scott, *J. Nucl. Mater.* 97 (1981) 337.
- [40] H.W. Weber, F. Nardai, C. Schwinghammer and R.K. Maix, *IEEE Trans. Magn.* MAG-17 (1981) 1711.
- [41] H.W. Weber, F. Nardai, C. Schwinghammer and R.K. Maix, *Adv. Cryogenic Engng.* 28 (1982) (in press).
- [42] M. Söll, C.A.M. van der Klein, H. Bauer and G. Vogl, *IEEE Trans. Magn.* MAG-11 (1975) 178.
- [43] M.A. Kirk and L.R. Greenwood, *J. Nucl. Mater.* 80 (1979) 159.
- [44] M. Söll, S.L. Wipf and G. Vogl, *IEEE Publ.* 72CH0682-5-TABSC (1972) 434.
- [45] M. Couach, J. Doulat and E. Bonjour, *IEEE Trans. Magn.* MAG-11 (1975) 170.
- [46] E.J. Kramer, *Adv. Cryogenic. Engng* 28 (1982) (in press).
- [47] P.S. Swartz, H.R. Hart and R.L. Fleischer, *Appl. Phys. Lett.* 4 (1966) 71.
- [48] H.W. Weber, Ed., *Anisotropy Effects in Superconductors* (Plenum Press, New York, 1977).